Acarologia

A quarterly journal of acarology, since 1959
Publishing on all aspects of the Acari

All information:

OPEN ACCESS

Acarologia is proudly non-profit,
with no page charges and free open access

Please help us maintain this system by
encouraging your institutes to subscribe to the print version of the journal
and by sending us your high quality research on the Acari.

Variation in the trophic morphology of Astigmatid mites common in UK beehives

Clive Bowman [ID] [a]

[a] Mathematical Institute, University of Oxford, Oxford, OX2 6GG, United Kingdom.

ABSTRACT

The chelal moveable digit in *Carpoglyphus lactis* (Linnaeus), *Glycyphagus domesticus* (DeGeer), and *Tyrophagus putrescentiae* (Schrank) from UK beehives is described using quantitative measures within a 2D mechanical model. The location of maximum jerk on the profile of the chelal moveable digit indicates the end of the mastication surface, which in these mites is confirmed to be just before the theoretical cut-off point for a functioning chewing 'machine'. All three species should be able to grasp yeasts, spores and mycelial hyphae in the hive. The moveable digit of *C. lactis* may be designed to enable pollenophagy. The mastication surface is 21.3 μm in *C. lactis*, 18.8 μm in *G. domesticus*, and 17.2 μm in *T. putrescentiae*. The wild-collected *C. lactis* shows the smallest chelal moveable digit tip velocity ratios (i.e., the lowest relative length of input to output moment arms). *Glycyphagus domesticus* has the most primitive geometry of its chela. The depth of the moveable digit matches the inferred resistive forces applied by the mite to food at that point. Condylar and moveable digit strengthening by sclerotisation is associated with eating tougher food. Effective chelal gape is 28.7 μm in *C. lactis*, 25.9 μm in *G. domesticus* and 24.8 μm in *T. putrescentiae*. Maximum food fragment size grabbed by the chela is estimated as 7786 $μm^3$ in *C. lactis*, 5348 $μm^3$ in *G. domesticus* and 4703 $μm^3$ in *T. putrescentiae*. Morsel size pre-ingestion is estimated as 4031 $μm^3$ in *C. lactis*, 5228 $μm^3$ in *G. domesticus* and 4246 $μm^3$ in *T. putrescentiae*. Under reasonable assumptions one of these mites might be able to excavate its own body volume equivalent in about one hour.

Keywords Astigmata; digging; functional ecomorphology; mechanics

Introduction

Three free-living astigmatid mite species can be found co-occurring in UK beehives: *Carpolyphus lactis* (Linnaeus) (Carpoglyphidae), *Glycyphagus domesticus* (De Geer) (Glycyphagidae), and *Tyrophagus putrescentiae* (Schrank) (Acaridae). In terms of comparative idiosomal size across a wide variety of free-living forms, Bowman (2021c) categorised all three of these as having an interstitial, potential cavity-living habit. Zoology is beset by 'just-so stories' whereby observational claims are made in support of various philosophies. As Akimov (1985) outlines, mite cheliceral chelae as tools differ in gross form, which may or may not be related ecomorphologically to particular lifestyles. What is crucially important in accepting any such explanations is that quantitatively they make sense. That is, the physical working of features is numerically consilient with any posed function. As Gebeshuber and Gordon (2011) says: "…biologists have changed, and the way they approach their science is getting closer and closer to the world of engineers, in terms of concepts, language and methods".

Robaux *et al.* (1977) reported *T. putrescentiae* to be an excavating geophage. The question arises that if all free-living astigmatids use their cheliceral chelae to do such digging, how big a bite could each species take? Furthermore, for any of an interstitial, potential cavity-living

habit, how long is such a mite likely to take to dig out a hole large enough to hide in? This requires one to estimate: the span (i.e., the effective gape) of a maximally open chela, the size of the mastication surface with which the moveable digit rests upon any material and generates friction, and the bite size when a moveable digit surface grasps into material. A check will also be made that variation in these parameters is consilient with previous attribution of feeding design using the ontology of Fashing (1998) and thus if the three co-occurring species could avoid trophic competition by mechanical design.

Material and methods

Preserved slide material of independently determined *C. lactis*, *G. domesticus* and *T. putrescentiae* collected from a single hive habitat in Redland, Avon, BS6 7JP, UK in 1983 deposited at Pest Infestation Control Laboratory, Slough was accessed by the author totalling 52 female specimens. Individuals of: *C. lactis* were "with sticky wetness" on 9th April, *G. domesticus* were "on surfaces" on 9th and 10th April, and *T. putrescentiae* were "under propylis/wax" on 10th April, all in the bee-nest (= brood box).

Drawings of each mite and its chelicerae (and for *T. putrescentiae* the lengths of its D1, D2 and L2 idiosomal setae) were made from all cleared mounted specimens using Nomarski interference phase-contrast microscopy with a drawing tube and micrometer scale. Idiosomal index (Lynch 1989) in μm was measured throughout and denoted IL. The lengths of dorsal setae (D1, D2, L2 – Griffiths *et al.* (1990)) were measured in μm for *T. putrescentiae* in order to determine Don Griffiths' likely breeding group using the classifier from Bowman (2021b). *Tyrophagus putrescentiae* 'B' is now assumed to be almost certainly the less commonly occurring close relative *Tyrophagus fanetzhangorum* Su *et al.*, 2020, but definitive identification of voucher specimens already deposited in museums (see Acknowledgments in Bowman (2021c)) is awaited. *Tyrophagus putrescentiae* 'A' (the 'commonly occurring form') retains its original name in this investigation following Klimov and OConnor (2009, 2010, 2015) and is not renamed as *Tyrophagus communis* Fan et Zhang, 2007. Individuals denoted as 'B' or 'A/B' (i.e., those individuals when the classifier based upon setal lengths on one side of the mite disagreed with the conclusions for setal length on the other side) were excluded from the analysis as mixed populations in the 'wild' may occur (Erban *et al.* 2016).

Drawings were scanned using a HP OfficeJet Pro 8720 and digitised measurements of: IL, setal lengths D1, D2 and L2; chelal design (L1U, L2M, CHI, CLI following (Bowman 2021c); and, cheliceral dentition [x,y] profiles with respect to the condyle-to-tip L2M axis were made using ImageJ 1.51s ex National Institutes of Health USA (available from http://imagej.nih.gov.uk/ij). Mite chelae were orientated by reflection and rotation such that their adductive lever moment arm directions (i.e., L2M see Bowman (2021c)) were aligned. Two fixed homologous features (the moveable digit tip and the fixed digit to moveable digit articulating condyle) were used for registration (Figure 1) i.e., the L2M axis is the 'reference line'. One landmark, the moveable digit tip, labeled (1) plus seventeen semi-landmarks (labeled 2–18) were determined by first scaling each L2M axis to the same size (rooted on the condyle) and then overlaying a equi-spaced 2D grid in order to digitise the moveable digit profile (black line in Figure 2) at standard increments along the L2M axis. Semi-landmark 18 was that directly vertical above the centre of the condyle seen laterally. This was not necessarily exactly where the adductive tendon inserts into the 'coronoid process' of the moveable digit (that is the length of y_{18} after undoing the rescaling does not necessarily match L1U). The moveable digit tip was taken to be the origin i.e., [x=0, y=0]. It is understood that a grid space of 1 indicates a slightly different actual spacing in μm for different specimens, but this is not about defining universal landmarks rather it is to deploy digit length adjusted semi-landmarks comparable across chelal designs.

Analyses were done in Excel2011 and R version 3.4.4 (2018-03-15) using untransformed data. Heat-maps and 3D plots used Graphis 2.7.3. Illustrations of the physics involved use the larger female *Tyrolichus casei* (Oudemans) cheliceral chela for clarity of exposition.
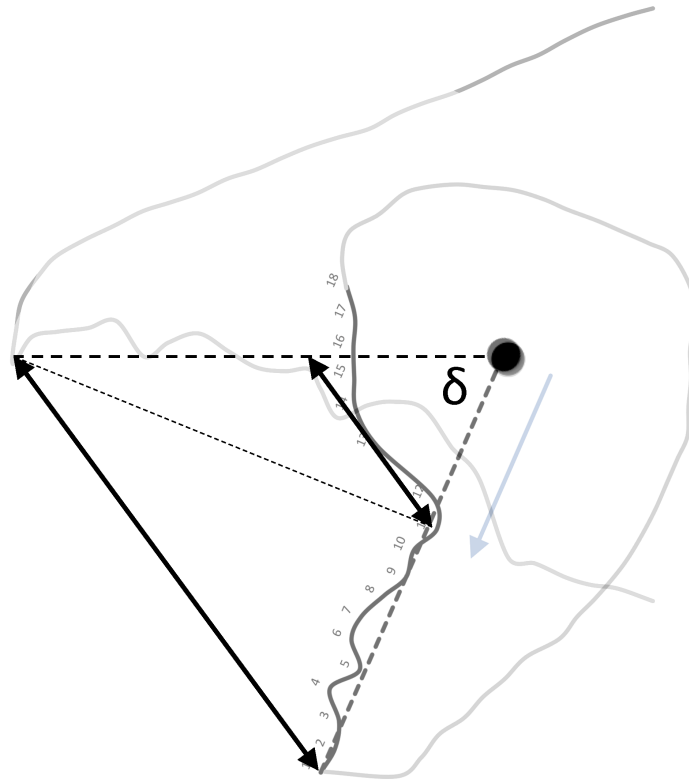
Figure 1 Maximum and minimum gripable fragment or morsel depth (when chela at maximum effective gape) indicated by solid double headed arrows. Maximum effective gape G is the fine dotted line from end of mastication surface on moveable digit to fixed digit tip. Grey arrow is of length equivalent to L1U from the condyle.

Chelal velocity ratio

The velocity ratio (= the ideal mechanical advantage) at the cheliceral chelal tip of the moveable digit (VR_{tip}) was calculated as $\frac{L1U}{L2M}$ (i.e., the length of the input moment arm divided by the length of the output moment arm of the closing adductive lever (Bowman 2021a)). No adjustment for adductive tendon angle was made.

End of mastication surface

The start of the chelal mastication surface, was taken to be the tip of the moveable digit, [x_1,0]. Jerk along the profile [x,y], i = 1…18 was estimated by

$$\frac{d^3y}{dx^3} = \frac{c_{i+1} - c_{i-1}}{x_{i+1} - x_{i-1}}, i = 4...15$$

where

$$c_i = \frac{d^2y}{dx^2} = \frac{g_{i+1} - g_{i-1}}{x_{i+1} - x_{i-1}}, i = 3...16$$

and

$$g_i = \frac{dy}{dx} = \frac{y_{i+1} - y_{i-1}}{x_{i+1} - x_{i-1}}, i = 2...17$$

The end of the mastication surface (e) equalled that x_i where $jerk_i$ or c_i was at a maximum, given y_i thereafter was monotonically increasing.
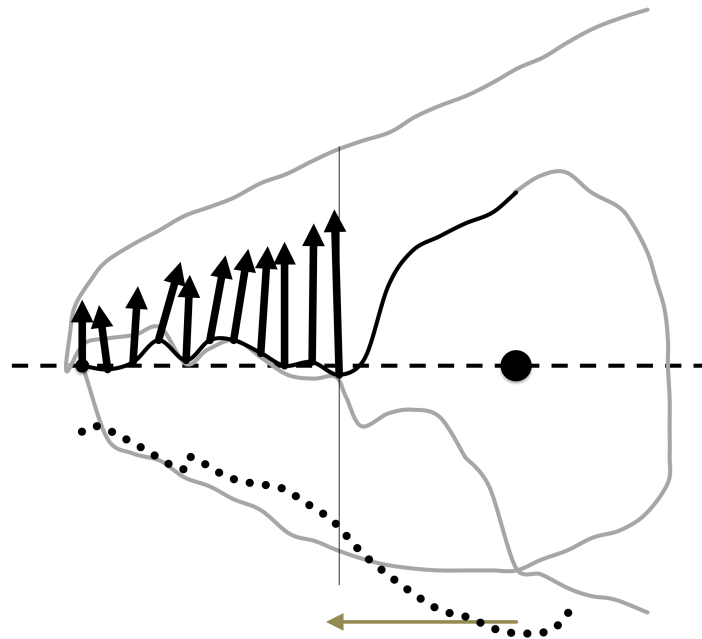
Figure 2 Adductive force vectors for unit F1 force on input moment arm tendon at each dentition feature on moveable digit. Bold black arrows show relative force sizes for each semi-landmark location along mastication surface at x_i, i = 1...11. Vertical line at i = 11 signifies end of mastication surface at essentially x = L2M-L1U. Dotted line is smoothed line through reflection in L2M axis of the tips of force (F2 = F1 * VR_i) arrows - showing how the moveable digit vertical form (its depth) is in proportion to the opposable forces it experiences on crushing food.

Span of moveable digit

The span of the moveable digit (or maximum effective chelal gape) is that distance from the end of moveable digit mastication surface to the fixed digit tip where any force at the end of moveable digit mastication surface is resisted by the fixed digit tip i.e. $G = L2M * sin(\delta)$. That is, given that the chelal tips meet, it is commensurate with a force orthogonal to L2M being applied (see Figure 1).

Sclerotisation/strengthening

The degree of comparative strengthening by sclerotisation of the condyle and of the moveable digit was scored numerically on a subjective scale (0 = not or feebly sclerotised, 1 = pale but sclerotised, 2 = brown moderately well sclerotised, 3 = dark brown heavily sclerotised) using specimens from Bowman (2021c). Inferred resistive forces at $[x_i, y_i]$ were calculated as $F1 * VR_i$ using F1 values from Bowman (2021c).

Maximum food fragment size grabbed

The difference between the digit tips at the maximum effective gape angle $\delta = cos^{-1} \frac{L2M}{(L2M - x_{ie})}$ in Figure 1 defines the maximum size of a foodstuff fragment that can be grabbed $= 2 * L2M * sin(\frac{\delta}{2})$ by the chelal digit tips, together with the consequent minimum fragment size $= 2 * (L2M - x_{ie}) * sin(\frac{\delta}{2})$ gripped by the end of the moveable digit mastication surface and its opposing fixed digit features proximal to the condyle. Note the maximum size > G always, and the minimum grazes the leading edge of the coronoid process (ascending ramus).

Astigmatid chelicerae work independently, taking it in turns to grab food-stuff and on retraction chopping it either side with the gnathosomal rutella before ingestion. An estimate of

food fragment volume Mv_G of a bite or 'grab' at the maximum effective gape G (see Figure 1) that could be gripped before any such truncation, would be by taking a cone of 2D apex angle δ and side length L2M and to subtract away a similar cone of side length $L2M - x_{ie}$. That is under the Trapezoidal rule, $= \frac{\Pi}{3} * (sin\ (\frac{\delta}{2}) * \frac{sin(\delta)}{2}) * (L2M^3 - (L2M - x_{ie})^3)$. This is an overestimate as although chelicerae can be approximated as cylinders, the chelal digits themselves are somewhat flattened. It also infers that the lateral truncation of grasped food preferentially occurs distal to the condyle. It represents the maximum chunk that might be torn away by a bite from that mite's single chelicera.

Morsel size pre-ingestion

If the thickness (denoted *thick*) in μm of chelal digits were known then an estimate of food fragment size after hypostomal truncation (= pre-ingestion morsel size) would be $= (thick) * \frac{sin(\delta)}{2} * x_{ie} * ((2 * L2M) - x_{ie})$ assuming that the rutella are held running along either side of the digits.

Digit effective thickness might be estimated basally at the condyle (= a constant spacing between the rutellae) or distally at the tip (i.e., the rutellae flexibly press outwards during cheliceral protrusion and then press inwards on retraction so that the minimum gap is the important parameter). Taking the first approach, Mariana *et al.* (2007) shows a SEM of *Blomia tropicalis* gnathosoma end-on from the front. From this, the ratio of moveable digit width (basally near the estimated position of the condyle) to cheliceral width (basally) can be estimated as 0.29. This closely agrees with Murillo *et al.* (2014) where for *T. putrescentiae* the ratio is approximately 0.28. Using digit thickness at the condyle as indicative of food fragment width after truncation by the rutellae appears reasonable (rather than using the digit width distally) when for instance the magnitude of the intra-pedipalp gap is considered (see gnathosoma of *Rhizoglyphus echinopus* ventrally in Hammen (1989) illustrated in Wirth (2006)).

Food fragments are dragged alternately by each chelicera into the labral area between the palps. The equivalent ratios for *A. siro* and *A. gracilis* in Iraola *et al.* (2015) were estimated as 0.29 and 0.32 respectively. However, Ahamad *et al.* (2011) shows an SEM of *Suidasia pontifica* where this ratio could be estimated somewhat higher at 0.39. Taking the cheliceral digit thickness estimated from various not quite 'face-on' scanning electron micrographs of another 46 astigmatid gnathosomal exemplars found on Internet web pages (covering *A. siro*, 'cheese-mite', '(house) dust mites', *Schwiebia* sp., and 'unknown') yields an average figure of 0.36. Combining these with the named examples in the above papers yields a consensus estimate of 0.35. This compares favourably with that of the highly derived astigmatids living in water-filled treeholes by Fashing (1998). That paper yields an estimate of 0.37 for *Naiadacarus arboricola* (although that for *Algophagus pennsylvanicus* at 0.50 is somewhat higher).

Bowman (2021a) suggests that the width of cheliceral segments are about 0.85 times the height of cheliceral segments i.e., they are sub-cylindrical. Accordingly for this study herein (where CHI was measured on each specimen), moveable digit thickness (*thick*) is estimated as $= 0.85 * 0.35 * CHI = 0.298 * CHI$.

Results

Mean (and sd) values for the lengths in μm of idiosomal setae in the 17 *T. putrescentiae* female individuals were: D1 43.1 (5.72), D2 127.5 (14.64), L2 43.3 (6.11). Table 1 summarises the chelal results.

Chelal velocity ratio

The wild-collected *C. lactis* shows the lowest chelal velocity ratio, *T. putrescentiae* the highest. *G. domesticus* has the most primitive geometry of its chela in that, unlike the other two species,

Table 1 Data table including summary mean and sd per species found in UK beehive. indicates specimen with inconsistent profile jerk criteria. Idiosomal length (IL), cheliceral length or reach (CLI), L2M or output moment arm condyle to moveable digit tip, L1U or input moment arm condyle to adductive tendon attachment point, location of end of mastication surface along L2M x_{ie}, m or length of mastication surface, G maximum effective gape (or span of moveable digit), and thickness of moveable digit (*thick*) at condyle in μm. Semi-landmark number i_e is nominal where 1=moveable digit tip. Velocity ratio of moveable digit tip, distance from condyle to end of mastication surface in L1U units and equivalent number of bite/grab are dimensionless. Delta (δ) is in degrees and adjusted for the measured (not the notional) location of the end of mastication surface. Max volume of bite/grab M_{vG}, food fragment truncated volume (pre-ingestion morsel size) TM_{vG}, and estimated idiosomal volume are in μm³. Excavation equivalent times are in mins.

Taxon	IL	CLI	L2M	L1U	VRtip	ie	Distance of ie from condyle in L1U units	xie	m	delta	G	CHI	*thick*	MvG	Estimated idiosomal volume	No. of bite/grab equivalents	Excavation time equivalents
Carpoglyphus lactis																	
224(1)-1 *	227.9	93.3	27.4	10.3	0.376	13	0.79	19.3	21.1	73	26.2	34.1	10.1	5932	18593014	3134	52
224(1)-5	264.3	103.2	30.9	9.6	0.309	13	1.01	21.3	23.4	72	29.4	34.2	10.2	8393	29010163	3457	58
224(1)-6 *	240.9	94.2	30.9	9.7	0.315	12	1.13	20.0	21.7	69	28.9	35.0	10.4	7880	21965011	2787	46
224(1)-6a	222.1	92.1	30.6	8.1	0.266	12	1.33	19.8	21.2	69	28.7	35.9	10.7	7663	17198826	2244	37
224(1)-6b	233.4	95.4	30.4	8.6	0.284	13	1.02	21.6	21.9	73	29.1	36.1	10.8	8157	19963051	2447	41
224(1)-6c	242.2	92.4	30.0	10.1	0.336	12	1.09	19.1	20.6	69	28.0	30.3	9.0	7093	22320579	3147	52
224(1)-10	229.2	92.2	28.6	10.7	0.373	13	0.77	20.3	22.4	73	27.4	37.1	11.1	6828	18908279	2769	46
224(1)-11 *	247.1	102.5	36.1	9.7	0.270	12	1.32	23.2	24.0	69	33.7	31.6	9.4	12440	23700819	1905	32
224(1)-11a	231.4	94.2	28.0	10.3	0.367	13	0.82	19.6	20.8	72	26.7	35.1	10.5	6280	19456566	3098	52
224(1)-11b	246.0	94.1	28.7	9.0	0.314	13	0.93	20.3	21.8	73	27.4	36.6	10.9	6836	23393715	3422	57
224(1)-11c	242.7	99.8	31.1	10.6	0.342	12	1.04	20.1	21.8	69	29.1	33.2	9.9	8004	22468395	2807	47
224(1)-12	237.7	94.3	30.5	9.5	0.313	12	1.14	19.7	21.9	69	28.5	33.1	9.9	7520	21087649	2804	47
224(1)-12a	254.6	98.8	34.8	11.3	0.325	12	1.09	22.5	22.9	69	32.5	39.2	11.7	11204	2593973	2315	39
224(1)-13 *	224.6	89.6	29.8	7.7	0.258	12	1.40	19.0	20.0	69	27.8	34.6	10.3	6945	17797823	2563	49
224(1)-13a	229.2	92.1	30.2	7.5	0.247	11	1.64	18.0	18.5	66	27.6	35.0	10.4	6718	18919758	2816	47
224(1)-15	239.6	89.7	31.0	9.1	0.293	12	1.25	19.6	20.2	69	28.8	33.2	9.9	7738	21616585	2793	47
224(1)-15a *	237.9	93.3	30.6	7.6	0.249	12	1.42	19.8	20.9	69	28.8	37.3	11.1	7653	21146371	2763	46
224(1)-15b *	235.1	94.8	33.2	9.6	0.289	11	1.43	19.4	20.5	66	30.2	37.8	11.3	8734	20403765	2336	39
224(1)-16	244.3	97.7	31.3	10.4	0.332	12	1.10	19.9	20.5	69	29.2	31.9	9.5	8050	22903188	2845	47
224(1)-18	235.1	99.9	30.8	11.6	0.375	13	0.79	21.7	22.7	73	29.4	39.0	11.6	8442	20401985	2417	40
224(1)-19	217.8	85.8	26.5	7.4	0.280	12	1.23	17.3	18.5	70	24.9	32.0	9.5	5006	16225261	3241	54
Summary	237.3	94.7	30.5	9.4	0.310	12	1.13	20.1	21.3	70	28.7	34.9	10.4	7786	20003561	2767	46
	10.9	4.3	2.2	1.3	0.042	1	0.24	1.4	1.4	2	1.9	2.4	0.7	1628	4848447	400	7
Glycyphagus domesticus																	
224(2)-1	243.7	123.9	33.5	14.3	0.426	9	1.23	16.0	21.1	58	28.6	65.1	19.4	7037	22735278	3231	54
224(2)-2	203.9	107.7	28.7	13.4	0.467	10	1.01	15.1	20.1	62	25.3	60.6	18.1	5026	13309677	2648	44
224(2)-3	242.5	114.9	31.9	14.5	0.456	9	1.16	15.0	17.5	58	27.0	64.6	19.2	5925	22409230	3782	63
224(2)-4	238.0	123.5	30.4	12.5	0.410	10	1.16	16.0	20.4	62	26.8	63.7	19.0	5934	21177842	3569	59
224(2)-5 *	183.6	115.7	31.5	11.4	0.360	10	1.33	16.4	22.3	61	27.7	56.0	16.7	6549	9716928	1484	25
224(2)-6	195.9	106.1	27.0	15.0	0.553	10	0.85	14.3	17.2	62	23.8	63.9	19.0	4183	11800938	2821	47
224(2)-7	212.9	108.0	26.6	13.6	0.513	10	0.92	14.1	18.5	62	23.5	58.7	17.5	4012	15160442	3779	63
224(2)-8	198.7	107.4	27.6	13.6	0.494	10	0.97	14.3	17.6	61	24.2	60.5	18.0	4356	12327158	2830	47
224(2)-9	204.8	115.5	33.5	14.9	0.445	8	1.31	14.0	16.9	54	27.2	58.3	17.4	5877	13491336	2296	38
224(2)-9a	211.4	111.2	31.8	16.5	0.518	9	1.03	14.9	17.1	58	26.9	62.7	18.7	5871	14831767	2526	42
224(2)-10	193.5	110.2	28.9	11.4	0.395	10	1.18	15.4	20.0	62	25.6	54.0	16.1	5202	11378467	2187	36
224(1)-20 *	210.3	110.1	29.2	13.6	0.466	9	1.14	11.9	17.1	58	24.7	58.1	17.3	4201	14599518	3476	58
Summary	211.6	112.9	30.1	13.7	0.459	10	1.11	14.8	18.8	60	25.9	60.5	18.0	5348	15244882	2886	48
	19.8	6.0	2.4	1.5	0.056	1	0.15	1.2	1.9	3	1.7	3.6	1.1	1004	4430570	709	12
Tyrophagus putrescentiae																	
224(1)-2	202.8	90.0	22.3	10.4	0.466	11	0.87	13.3	14.8	66	20.4	45.8	13.7	2710	13102202	4836	81
224(1)-3	221.7	101.0	31.4	14.9	0.473	10	0.98	16.9	19.7	62	27.9	55.0	16.4	6724	17105341	2544	42
224(1)-4 *	252.8	100.8	28.5	13.1	0.459	9	1.17	13.2	16.5	57	24.0	55.8	16.6	4130	25373674	6144	102
224(1)-5a	279.4	104.7	31.0	15.0	0.484	9	1.11	14.4	18.5	58	26.2	58.4	17.4	5401	34271226	6345	106
224(1)-6	244.2	93.9	27.7	12.1	0.437	9	1.20	13.1	17.0	58	23.6	50.7	15.1	3936	22880842	5813	97
224(1)-6a *	281.4	108.3	30.2	13.7	0.454	9	1.17	14.2	17.5	58	25.6	61.7	18.4	5035	34995020	6950	116
224(1)-7 *	250.4	104.8	28.3	12.1	0.428	10	1.10	14.9	18.1	62	25.0	55.2	16.4	4825	24666156	5112	85
224(1)-7a	238.5	92.6	25.6	11.8	0.459	10	1.02	13.7	15.2	62	22.7	50.6	15.1	3619	21309015	5887	98
224(1)-7b	309.0	105.2	32.2	15.1	0.469	9	1.12	15.3	17.7	58	27.4	56.7	16.9	6170	46324163	7508	125
224(1)-7c *	237.3	91.5	26.8	14.2	0.531	9	1.00	12.6	15.0	58	22.7	48.8	14.5	3519	20979594	5962	99
224(1)-7d *	257.9	101.1	29.4	14.1	0.480	9	1.11	13.7	17.5	58	24.9	56.6	16.9	4629	26937660	5820	97
224(1)-8a	269.3	108.5	30.8	15.4	0.501	10	0.93	16.4	19.0	62	27.3	56.3	16.8	6293	30666449	4873	81
224(1)-8b *	255.7	102.5	33.3	15.0	0.452	8	1.30	13.6	16.6	54	26.9	51.8	15.4	5599	26250077	4688	78
224(1)-10 *	234.6	93.4	24.9	12.0	0.481	10	0.97	13.2	15.9	62	22.0	43.5	13.0	3302	20289879	6145	102
224(1)-10a	248.1	96.6	26.2	13.7	0.523	11	0.78	15.5	18.7	66	23.9	48.5	14.5	4356	24001068	5510	92
224(1)-14	264.8	104.1	33.5	14.3	0.428	8	1.36	14.0	17.3	54	27.3	56.2	16.8	5881	29158040	4958	83
224(1)-odd2 *	253.6	99.8	26.2	13.2	0.505	8	0.93	13.9	16.6	62	23.1	51.6	15.4	3826	25624011	6697	112
Summary	253.0	99.9	28.7	13.5	0.472	9	1.07	14.2	17.2	60	24.8	53.1	15.8	4703	26113789	5635	94
	24.3	5.9	3.2	1.4	0.030	1	0.15	1.2	1.4	4	2.2	4.8	1.4	1170	7649293	1119	19

the attachment point for the adductor tendon with the basal coronoid process of the moveable digit is posterior of the condyle as illustrated for *Chortoglyphus arcuatus* in Akimov and Gaichenko (1976). This would be an interim state in the evolution of the chela from a simple appendage if it follows the same process as in other jaws (DeMar and Barghusen 1973).

End of mastication surface

The location of maximum jerk on the profile of the chelal moveable digit indicated the end of the mastication surface. In a few mites (marked with *) this was inconsistent and the end of mastication surface was taken to be the semi-landmark before that showing maximum curvature. Overall, the end of the mastication surface is confirmed to be just before the theoretical cut-off point for a functioning chewing 'machine' (i.e, where the velocity ratio would be =1).

Span of moveable digit

The largest and smallest span of the moveable digit surface which can grasp material (i.e., the largest and smallest effective gape of a maximally open chela) are respectively, 28.7 μm (*C. lactis*) and 24.8 μm (*T. putrescentiae*). Note that although the adductive muscle tendon (inserting around semi-landmark 18 and pulling approximately parallel to L2M axis – would have to flex around it), the coronoid process does not impinge internally upon the dorsum of the chelal shaft. Forces for moveable digit features distal of the end of the mastication surface when maximally open would have no opposition from the fixed digit.

Free-living astigmatids in being saprophagous must be challenged to eat nematodes, nematode eggs, fungal spores and hyphae along with their base foodstuff in the wild (even in beehives). Figure 3 shows values of average x_{ie} for the wild-collected samples of the three taxa versus the typical sizes for spore, fungal, yeast, plant and animal cells.

Fungal spores vary in general size from 2 to ≈ 100 μm (illustrated in Golan and Pringle (2017)) although some can be as large as 250 μm (Gehring *et al.* 2002). Most typical soil fungal spores (and even small protists (Luan *et al.* 2020)) therefore could be grasped by the chela of all three mite species. Fungal (mycorihizal) hyphae are commonly 5−10 μm but can be as small as 3−8 μm in diameter (Dodd *et al.* 2000). Therefore, the chela of the three UK beehive-living species could grab these too. Note that in extreme cases fungal hyphae can be even as low as 2 μm in size or as large as 1 mm. Protozoa, rotifers, tardigrades and nematodes are 4−200 μm in size meaning that some of these could be grasped (even anecdotally) by these astigmatids. Soil nematodes are non-segmented worms typically 50 μm (range 15–100 μm) in diameter. Some of these (< 20 μm diameter) could be grasped by the scale of mastication surfaces in the three UK beehive species. Entomophagous nematodes are known to attack astigmatids (Nermut *et al.* 2019). Their use in plant protection can expose bees to them (Erler *et al.* 2022). Plant parasitic worms can be much bigger, 2,000 μm or more in length (Stirling *et al.* 2002) and are thus unlikely to be consumed if accidentally found in the hive.

Carpoglyphus lactis as well as being a pest of stored products of high sugar content is strongly pollenophagous in the wild (Vijaykumar *et al.* 2013). Pollen has a high protein content (up to 35% (Anastasov 2022)) but in comparison to flower nectar or honey is poor in soluble carbohydrate content. The main group of carbohydrates are insoluble celluloses (up to 15.9% fibre content) and only small amounts of starch and sugars (Serra and Jorda 1977). Among angiosperm species, pollen grain diameter ranges from less than 10 μm (e.g., in forget-me-not, *Myosotis*) to over 100 μm (in some species like cotton or cucumber) (Hao *et al.* 2020). They are categorised as very small (< 10 μm), small (10−25 μm), medium (25−50 μm), large (50−100 μm), very large (100−200 μm), or giant (>200 μm) (Ferreira *et al.* 2020). So, considering the maximum effective gape of the three species herein they could only grasp small to medium grains like those of the common sunflower (*Helianthus annuus*) found in UK gardens (and thus in beehives), coriander, dill, and wild roses for instance (but not *Hibiscus* pollen, nor pollen from wheat (Golan and Pringle 2017)). Ragweed pollen at 17−23 μm could only be grabbed by *C. lactis* at best. Pollen grains of lucerne, various clovers and ornamental trees such as the Judas
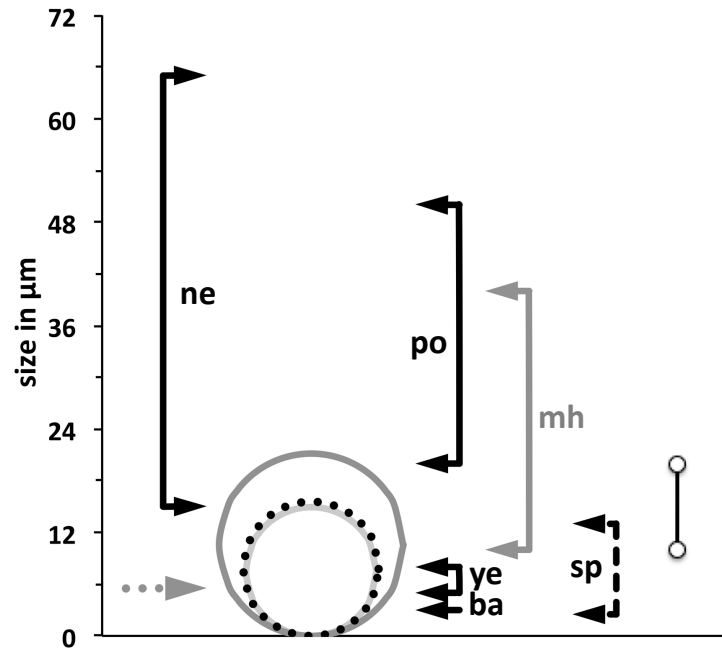
Figure 3 Average mastication surface length along L2M axis (x_{ie} in μm) as a circle for UK beehive specimens of: *Carpoglyphus lactis* = dark grey outer circle; *Glycyphagus domesticus* = dotted circle; *Tyrophagus putrescentiae* = inner pale grey circle; compared to range of diameters of typical food-stuffs. ne = soil nematodes. po = pollen. mh = mould hyphae. sp = spores. ye = yeasts. b = bacteria. Dashed grey arrow on left is span of three small teeth on *C. lactis* moveable digit proximal to condyle. Line ended with open circles = dust mite faeces for comparison. Typical diameters in μm are: human hair 80; grain of salt 60−100; *Paramecium* 50−330; carrot cells 40−75; red blood cells/human dander/fine floor dust 40; white blood cells 20; plant & animal cells 10−100; talcum powder/heavy dust 10; wood smoke 3; clouds, fog, sea spray and mineral dust 1−100; light dust/animal dander 1−5. The limit of visibility of particles visible to the naked eye is around 25−40 μm. Note that the moveable digit mastication surface ('drape distance') *m* will be greater as it allows for surface asperities and gullets.

tree or the Black locust tree could be almost grasped by the chela of all three mites. However, for most plant species, most individual pollen grains are actually small to medium (ca. 20–40 μm) in size which then precludes the tyrophagid and glycyphagid herein from grasping them whole. Perhaps these taxa scrape off the oily 'pollenkitt' with its high content of fats and fatty acids (Serra and Jorda 1977) that cover the pollen grains instead when in the hive.

Even though the elongate digit of *C. lactis* is suitable for pollenophagy, note that even *C. lactis* does not have the cheliceral tip design of an old fashioned 'stab can-opener' like in some pollenophagous phytoseiids (Adar *et al.* 2012). In those mesostigmatids the fixed digit may hold the pollen down against the substrate and the moveable digit repeatedly slices into it by leverage. As among angiosperm species, pollen grain volume ranges over almost five orders of magnitude (Hao *et al.* 2020) and common pollens like from Mary thistle, caper spurge, white flax, blue flax, safflower, sesame, oil pumpkin and oil gourd are too large to be grasped, if astigmatids repeatedly bite into and demolish these larger pollen grains this needs examining as to how in a SEM follow-up study.

Note that the distance along the L2M axis encompassing the three small posterior teeth in *C. lactis* at around 5.5 μm is just in excess of the 3 μm size of the largest soil bacteria (which are normally around 1 μm in size (Luan *et al.* 2020)) and of the order of the diameter of the smaller fungal hyphae (at 1–3 μm (Phillott and Parmenter 2006), or 2–5 μm (Bakken and Olsen 1983)). Yeast cells (present in beehives and tree exudates) vary enormously in size. However, although the largest yeast can be as big as 40 μm, the size of an average yeast cell is between 3 and 12 μm depending upon species, so could be grasped (cracked and sheared) by the chela of

all three of the species herein. *Tyrophagus putrescentiae* is known to feed upon various yeasts (and dermatophytes) (Duek *et al.* 2001).

Sclerotisation/strengthening

For *C. lactis* (Ca4) sclerotisation of the condyle and moveable digit scored 0 and 0, respectively. For *G. domesticus* (G5) sclerotisation of the condyle and moveable digit scored 3 and 3, respectively. For *T. putrescentiae* (T13) sclerotisation of the condyle and moveable digit scored 1 and 1, respectively. The depth of the moveable digit matches the inferred resistive forces applied by the mite to food at that point. Condylar and moveable digit strengthening by sclerotisation is associated with eating tougher food (as indicated by the F2 values).

Size of the mastication surface

The largest and smallest size of the mastication surface with which the moveable digit can rest upon any material and generate friction are respectively, 21.3 μm (*C. lactis*) and 17.2 μm (*T. putrescentiae*).

Maximum food fragment size grabbed

Maximum food fragment size grabbed by the chela is shown in Table 1. Comparing them to the overall gross gut bolus size in astigmatids yields useful insights. For instance, Hubert *et al.* (2004) illustrates a gastric bolus in *A. siro* of 11.4 μm diameter (thus approximately 782 μm^3 in volume). For *C. lactis*, Hubert *et al.* (2014) illustrate gastric boli of 20.1–35.1 μm diameter (equivalent to 531–2,830 μm^3 in volume). This overlaps with the scale of chelal gape in this species. On the face of it, only one maximum-gape grab of food material might yield the equivalent of a single gastric bolus in this so-called 'picking' species. Erban and Hubert (2010) illustrates gastric boli in *Dermatophagoides farinae* and *T. putrescentiae* of 60.0–65.0 μm and 14.7 μm diameter respectively (thus approximately 113,097–143,793 μm^3 and 1,665 μm^3 in volume respectively). The bolus in *T. putrescentiae* must comprise more than one cheliceral grab as it is much wider than the length of the mastication surface (at 17 μm). Its volume would be equivalent to at best one grabbing bite suggesting this mite is more of a grazer or shredder than a collecting picker. Note that the hole excavated by one 'bite' of the two chelicerae will be only somewhat larger than that for one chela due to the partial overlap of their calculated volumes (unless the mite moves its gnathosoma laterally between bites). Erban *et al.* (2016) illustrate *T. putrescentiae* with such gastric boli of 106.2–110.2 μm diameter (thus 627,995–701,398 μm^3 in volume). This would also infer that many bites are needed to produce this suggesting it is a grazer. Using a variety of approximations, Brown *et al.* (2016) suggests that the total volume of the nematode *Aplectus antarcticus* is 39,800–97,700 μm^3. This suggests that *T. putrescentiae* might be able to grab and tear into such sized worm-like prey if encountered in <100 chunks (if they can be partly grabbed – see above). More observations of *T. putrescentiae* feeding in the wild are needed.

Erban and Hubert (2011) states that food boli in *Lepidoglyphus destructor* are 80–100 μm in size. If this is a diameter then that suggests bolus volumes of 33,510–65,450 μm^3. Kopeck'y *et al.* (2014) illustrates the gastric boli of *L. destructor* of 25.7 μm diameter (thus approximately 8,896 μm^3 in volume). Hubert *et al.* (2019) also illustrates the gastric boli in *D. pteronyssinus* and *D. farinae* at 12.9–58.8 μm and 22.2–34.5 μm diameter respectively (thus approximately 1,121–106,675 μm^3 and 5,710–21,587 μm^3 in volume respectively). Follow-up work is needed to determine if glycyphagids and pyroglyphids are likely to be shredders or grazers based upon their bite/bolus volume ratio.

The body volume of an astigmatid can be conservatively approximated by a cylinder of idiosomal index in diameter and two times the idiosomal index in length i.e., body volume $= \frac{\Pi}{2} * IL^3$ (Table 1). At least *T. putrescentiae* is known to be a burrowing geophage constructing pores and aerating the substrate (Robaux *et al.* 1977). Indeed, Bowman (2021c) classifies it

(T13 'A') along with *C. lactis* (Ca4) as an 'Interstitial'. Potential cavity-living, substratum browsing / gleaning 'generalist' species. On the other hand *G. domesticus* (G5) was classified an 'Interstitial'. Potential cavity-living, possible crevice feeding / excavating 'specialist'. If these three species solely used their chelicerae to dig into food material with each chelicera grabbing and tearing off a chunk every second (that was then moved away backwards out of the way immediately by their pedipalps / legs) then a hole equivalent to their estimated body volume could be excavated by a single mite in around an hour or so (Table 1). This is reasonable to believe might happen and could be critically examined by timed observations of individual mites in a follow-up experiment. Noticeably small mites (i.e., subject to higher environmental temperatures (Bowman 2021b)) in theory could excavate a body-size equivalent hole even more quickly as volume is a cube relationship to length. This time could be shorter if the mite's legs are used as digging tools too.

Morsel size pre-ingestion

The thickness values (*thick*) are so small that the opportunity for wide transversal ridges on digit teeth that could act as 'crush-blades' of hard fibrous material like the molars of vertebrate ungulates (Schulz *et al.* 2010) is limited except at the nano-scale. This could be looked for in a follow-up SEM study. Note that the thickness at the condyle closely approximates the size of the input lever moment arm (L1U, Table 1) suggesting perhaps a growth process that is similar dorsoventrally as well as laterally during chelal evolution.

Morsel size pre-ingestion TMv_G figures per specimen are shown in Table 1. These morsel volumes could be compared to the typical fragment sizes found within the gastric boli of astigmatids as a validation in follow-up work. The lower limit of the measured gastric bolus volumes listed above at 1,121 μm³ (assuming that they are spherical) exceeds the size of: human sperm cells (30 μm³), red blood cells (100 μm³), lymphocytes (130 μm³), neutrophils (300 μm³) and beta cells (1,000 μm³). The range of measured gastric bolus volumes (up to 701,398 μm³) encompasses all other human individual cell volumes including fat cells at 600,000 μm³. Only, human oocytes at 4,000,000 μm³ are bigger. The bolus volumes are generally much larger than the truncated food fragment volumes calculated herein, thus needing multiple chelal grabs to form (given the wastage of material from trimming). However, some other sort of oral trituration process of grabbed food material must also be happening after the chelae engage and crush the food as many mite anatomists illustrate a tiny trans-neural mass oesophagus in acarines (of the order of 10–15 μm diameter, e.g., Alberti *et al.* (2003), Erban and Hubert (2011)) through which food must pass. This lumen width is only a little less than the average mastication surface length for the three species (see Table 1) so, perhaps, one chelal 'grab-length' of material might be directly ingested once the distal parts of torn-off morsel were further trimmed laterally and dorsoventrally. Hubert *et al.* (2014) do illustrate tiny food fragments much smaller than the bolus in the caecal lumen (approximately 0.5–2 μm in diameter i.e., around <5 μm³ in volume), so some sort of 'post-grab' processing must occur. These very tiny elements are at the scale of bacterial cells when accompanied by slime capsules (Bakken and Olsen 1983). The 'end-on' SEM of the gnathosoma of the water-filled tree-hole living *Naiadacarus arboricola* (i.e., Figure 4B in Fashing (1998)) suggests that distally the digits themselves on their own are only about half the width of their size at the condyle. Considering this as the effective 'trim width' would only reduce the estimates of the truncated food fragment size in by half (and thus divide the TM_G volume by eight in Table 1) if it was used above (rather than taking the digit width at the condyle). This is still insufficient to reduce the food sizes down enough for the smallest fragment sizes to be consilient with Hubert *et al.* (2014)'s photographs. i.e., even if the minimum gap between the rutella as the tips of the chelicerae digits passes between them is the important operating parameter. Further thought on a pre-ingestion trituration process of grabbed and trimmed food material (perhaps by a labrum) together with some gastric bolus forming assembly mechanism is needed. Griffiths (pers. comm.) maintained that material could be seen not just to be squeezed within the gut of astigmatids but also whirled around.

Discussion

The results are consilient with *C. lactis* being regarded as a fragmentary feeding 'picker/collector' species. That is, this UK beehive species could pick over surfaces with its long digits (of low VR_{tip} and large x_{ie}), then slice (due to its large m and low chelal *F2* force (Bowman 2021c)) the generally soft food that it collects, selectively squashing small harder elements into the smallest pre-ingestion morsels with its back teeth. The moveable digit of *C. lactis* is also designed to enable some degree of pollenophagy with its large maximum effective gape and large bite volume.

The results are consilient with *G. domesticus* being regarded as a pan-saprophagous 'shredder'. That is, a possible crevice feeding/excavating specialist species, crunching (using its large chelal *F2* force (Bowman 2021c)) both large and hard foodstuffs, resulting in the largest pre-ingestion morsel sizes of the three UK beehive species.

The results are consilient with *T. putrescentiae* being regarded as a burrowing 'browser/gleaner' generalist. That is, a fragmentary feeder with the smallest bite size of the three species, grabbing relatively small and relatively soft food morsels that are selectively squashed using its moderate chelal *F2* force (Bowman 2021c).

So, although all three species should be able to grasp yeasts, spores and mycelial hyphae in the hive (Figure 3), trophic competition could be avoided.

Acknowledgements

ORCID

Clive Bowman https://orcid.org/0000-0002-4558-4981

References

Adar A., Inbar M., Gal S., Doron N., Zhang X-Q., Palevsky E. 2012. Plant-feeding and non-plant feeding phytoseiids: differences in behavior and cheliceral morphology. Experimental and Applied Acarology, 58(4):341-357. https://doi.org/10.1007/s10493-012-9589-y

Ahamad M., Louis S.R., Hamid Z., Ho T.M. 2011. Scanning electron micrographs of medically important dust mite, *Suidasia pontifica* (Acari: Astigmata: Saproglyphidae) in Malaysia. Tropical Biomedicine, 28(2):275-282

Akimov I.A. 1985. Biological foundations of harmfulness in acaroid mites. Naukova Dumka, Kiev. pp. 160 (in Russian)

Akimov I.A., Gaichenko V.A. 1976. The principle of action of the claws of the chelicerae in mites of the families Acaridae Leach, 1816 and Glyciphagidae Berlese, 1923 in connection with their adaptation to different food substrates. Dopovididi Akademiyi Nauk Ukrayins'koy RSR, seriya B. Heolohichni, khimichni ta biolohichni nauky, 0(4):352-355 (in Russian)

Alberti G., Seniczak A., Seniczak S. 2003. The digestive system and fat body of an early-derivative oribatid mite, *Archegozetes longisetosus* Aoki (Acari: Oribatida, Trhypochthoniidae). Acarologia, 43(1-2): 149-219.

Anastasov A. 2022. The Nutritional Value of Pollen. BBKA News January 2022: 10-12

Bakken L.R., Olsen R.A. 1983. Buoyant Densities and Dry-Matter Contents of Microorganisms: Conversion of a Measured Biovolume into Biomass. Applied and Environmental Microbiology, 45(4):1188-1195 https://doi.org/10.1128/aem.45.4.1188-1195.1983

Bowman C.E. 2021a. Feeding design in free-living mesostigmatid chelicerae (Acari : Anactinotrichida). Experimental and Applied Acarology, 84(1):1-119. https://doi.org/10.1007/s10493-021-00612-8

Bowman C.E. 2021b. Could the acarid mite *Tyrophagus putrescentiae* (Schrank) be used as an environmental thermometer? International Journal of Acarology, 47(2):107-118. https://doi.org/10.1080/01647954.2021.1877350

Bowman C.E. 2021c. Cheliceral chelal design in Astigmatid mites. Experimental and Applied Acarology, 84(2):271-363. https://doi.org/10.1007/s10493-021-00625-3

Brown S., Pedley K.C., Simcock D.C. 2016. Estimation of Surface Area and Volume of a Nematode from Morphometric Data. Scientifica 2016, Article ID 6767538, 7 pp. https://doi.org/10.1155/2016/6767538

DeMar R., Barghusen H.R. 1973. Mechanics and the evolution of the synapsid jaw. Evolution, 26(4):622-637 https://doi.org/10.1111/j.1558-5646.1972.tb01969.x

Dodd J.C., Boddington C.L., Rodriguez A., Gonzalez-Chavez C., Mansur I. 2000. Mycelium of Arbuscular Mycorrhizal fungi (AMF) from different genera: form, function and detection. Plant and Soil, 226:131-151

Duek L., Kaufman G., Palevsky E., Berdicevsky I. 2001. Mites in fungal cultures. Mycoses, 44:390-394 https://doi.org/10.1046/j.1439-0507.2001.00684.x

Erban T., Hubert, J. 2010. Determination of pH in Regions of the Midguts of Acaridid Mites. Journal of Insect Science, 10(42):1-12. https://doi.org/10.1673/031.010.4201

Erban T., Hubert J. 2011. Visualization of protein digestion in the midgut of the acarid *Lepidoglyphus destructor*. Archives of Insect Biochemistry and Physiology, 78(2):74-86 https://doi.org/10.1002/arch.20441

Erban T., Klimov P.B., Smrz J., Phillips T.W., Nesvorna M., Kopecky J., Hubert J. 2016. Populations of Stored Product Mite *Tyrophagus putrescentiae* Differ in Their Bacterial Communities. Frontiers in Microbiology, 7, Article 1046, pp. 19. https://doi.org/10.3389/fmicb.2016.01046

Erler S., Eckert J.H., Steinert M., Alkassab A.T. 2022. Impact of microorganisms and entomopathogenic nematodes used for plant protection on solitary and social bee pollinators: Host range, specificity, pathogenicity, toxicity, and effects of experimental parameters. Environmental Pollution, 302:119051. https://doi.org/10.1016/j.envpol.2022.119051

Fan Q-H., Zhang Z-Q. 2007. *Tyrophagus* (Acari: Astigmata: Acaridae). Manaaki Whenua Press, Lincoln, New Zealand. pp. 291

Fashing N.J. 1998. Functional morphology as an aid in determining trophic behaviour: The placement of astigmatic mites in food webs of water-filled tree-hole communities. Experimental and Applied Acarology, 22:435-453 https://doi.org/10.1023/A:1006081622519

Ferreira C.T., Krug C., de Moraes G.J. 2020. Effect of pollen of different plant species on the oviposition of two phytoseiid mites (Acari: Phytoseiidae) commonly found in citrus orchards in the Brazilian Amazonia. Acarologia, 60(1):22-29. https://doi.org/10.24349/acarologia/20204360

Gebeshuber I.C., Gordon R. 2011. Bioinspiration for Tribological Systems on the Micro- and Nanoscale: Dynamic, Mechanic, Surface and Structure Related Functions. Micro and Nanosystems, 3:271-276 https://doi.org/10.2174/1876402911103040271

Gehring C.A., Wolf J.E., Theimer T.C. 2002. Terrestrial vertebrates promote arbuscular mycorrhizal fungal diversity and inoculum potential in a rain forest soil. Ecology Letters, 5:540-548 https://doi.org/10.1046/j.1461-0248.2002.00353.x

Golan J.J., Pringle A. 2017. Long-Distance Dispersal of Fungi. Microbiol Spectrum 5(4):FUNK-0047-2016, pp. 24. https://doi.org/10.1128/microbiolspec.FUNK-0047-2016

Griffiths D.A., Atyeo W.T., Norton R.A., Lynch C.A. 1990. The idiosomal chaetotaxy of astigmatid mites. Journal of Zoology, 220(1):1-32 https://doi.org/10.1111/j.1469-7998.1990.tb04291.x

Hammen L van der 1989. An introduction to comparative Arachnology. SPB Academic Publishing, The Hague. pp. 576

Hao K., Tian Z-X., Wang Z-C., Huang S-Q. 2020. Pollen grain size associated with pollinator feeding strategy. Proceedings of the Royal Society B, 287:20201191. https://doi.org/10.1098/rspb.2020.1191

Hubert J., Kudl'ikov'a I., Stejskal V. 2004. Review of digestive enzymes of stored product and house dust mites. Phytophaga, 14:695-710

Hubert J., Nesvorn'a M., Kopeck'y J., Erban T., Klimov P. 2019. Population and Culture Age Influence the Microbiome Profiles of House Dust Mites. Microbial Ecology, 77:1048-1066. https://doi.org/10.1007/s00248-018-1294-x

Hubert J., Nesvorn'a M., Kopeck'y J., Sagov'a-Marecˇkov'a M., Poltronieri P. 2014. *Carpoglyphus lactis* (Acari: Astigmata) from various dried fruits differed in associated micro-organisms. Journal of Applied Microbiology, 118:470-484 https://doi.org/10.1111/jam.12714

Iraola V., Prados M., Pinto H., Morales M., Leonor J.A., Carn'es J. 2015. Allergological characterisation of the storage mite *Acarus gracilis* (Acari: Acaridae). Allergologia et immunopathologia (Madrid), 43(4):332-338 https://doi.org/10.1016/j.aller.2014.04.004

Klimov P.B., OConnor B.M. 2009. Conservation of the name *Tyrophagus putrescentiae*, a medically and economically important mite species (Acari: Acaridae). International Journal of Acarology, 35:95-14 https://doi.org/10.1080/01647950902902587

Klimov P.B., OConnor B.M. 2010. Case 3501. *Acarus putrescentiae* Schrank, 1781 (currently *Tyrophagus putrescentiae*; Acariformes, ACARIDAE): proposed conservation of usage by designation of a replacement neotype. Bulletin of Zoological Nomenclature, 67(1):24-27 https://doi.org/10.21805/bzn.v67i1.a2

Klimov P.B., OConnor B.M. 2015. Comment on *Acarus putrescentiae* Schrank, 1781 (currently *Tyrophagus putrescentiae*; Acariformes, ACARIDAE): proposed conservation of usage by designation of a replacement neotype. Bulletin of Zoological Nomenclature, 72(1):50-56

Kopeck'y J., Nesvorn'a M., Hubert J. 2014. *Bartonella*-like bacteria carried by domestic mite species. Experimental and Applied Acarology, 64:21-32. https://doi.org/10.1007/s10493-014-9811-1

Luan L., Jiang Y., Cheng M., Dini-Andreote F., Sui Y., Xu Q., Geisen S., Sun B. 2020. Organism body size structures the soil microbial and nematode community assembly at a continental and global scale. Nature Communications, 11:6406. https://doi.org/10.1038/s41467-020-20271-4

Lynch C.A. 1989. Two new species of the genus *Tyrophagus* (Acari: Acaridae). Journal of Zoology, London, 219:545-567 https://doi.org/10.1111/j.1469-7998.1989.tb02600.x

Mariana A., Santana Raj A.S., Tan S.N., Ho T.M. 2007. Scanning electron micrographs of *Blomia tropicalis* (Acari: Astigmata: Echimyopodidae), a common house dust mite in Malaysia. Tropical Biomedicine, 24(2):9-37

Murillo P., Aguilar H., Sanchez E. 2014. Use of different SEM techniques in the study of *Tyrophagus putrescentiae* (Acari: Acaridae) in Costa Rica. UNED Research Journal / Cuader'nos de Investigaci'on UNED, 5(2):201-208 https://doi.org/10.22458/urj.v5i2.273

Nermut J., Zemek R., Mráček Z., Palevsky E, Půža V. 2019. Entomopathogenic nematodes as natural enemies for control of *Rhizoglyphus robini* (Acari: Acaridae)? Biological Control, 128:102-110. https://doi.org/10.1016/j.biocontrol.2018.10.003

Phillott A.D., Parmenter C.J. 2006. The ultrastructure of sea turtle eggshell does not contribute to interspecies variation in fungal invasion of the egg. Canadian Journal of Zoology, 84:1339-1344. https://doi.org/10.1139/z06-125

Robaux P., Jeanson C.Y., Barbier D. 1977. Microstructures construites par un acarien *Tyrophagus putrescentiae* dans une argile. Etude experimentale et microscopique. Ecological Bulletins 25, Soil Organisms as Components of Ecosystems, pp. 489-493, Oikos Editorial Office. https://www.jstor.org/stable/20112618

Schulz E., Calandra I., Kaiser T.M. 2010. Applying tribology to teeth of hoofed mammals. Scanning, 32(4)162-182. https://doi.org/10.1002/sca.20181

Serra Bobvehi J., Jorda R.E. 1977. Nutrient composition and microbiological quality of honey-bee collected pollen in Spain. Journal of Agriculture and Food Chemistry, 45:725-732 https://doi.org/10.1021/jf960265q

Stirling G., Nicol J., Reay F. 2002. Advisory Services for Nematode Pests. Operational Guidelines. Rural Industries Research and Development Corporation, Australia. Publication No. 99/41. Project No. AAN-2A. pp. 119

Su X., Fang Y., Xu J-Y., Fang W-X., Zhan X-B., Fang Y., Chu L-M., Feng R., Jin Y-L., Sun E-T. 2020. The complete mitochondrial genome of the storage mite pest *Tyrophagus fanetzhangorum* (Acari: Acaridae). Systematic and Applied Acarology, 25(9):1693-1701. https://doi.org/10.11158/saa.25.9.14

Vijayakumar K., Muthuraman M., Jayaraj R. 2013. Infestation of *Carpoglyphus lactis* (Linnaeus) (Acari: Carpoglyphidae) on *Trigona iridipennis* (Apidae: Meliponinae) from India. Scholarly Journal of Agricultural Science, 3(1):25-28

Wirth S. 2006. Morphology and function of the gnathosoma in the Histiostomatidae (Astigmata). Acarologia, 46(1-2):103-109